Unusual double-peak specific heat and spin freezing in a spin-2 triangular lattice antiferromagnet FeAl₂Se₄

Kunkun Li[1,2], Shifeng Jin[1,3], Jiangang Guo[1], Yanping Xu[1], Yixi Su[5], Erxi Feng[5], Yu Liu[6], Shengqiang Zhou[6], Tianping Ying[7], Shiyan Li[7,9,10], Ziqiang Wang[11,*], Gang Chen[7,8,10,†] and Xiaolong Chen[1,3,4‡]

[1]*Research & Development Center for Functional Crystals,*
Beijing National Laboratory for Condensed Matter Physics,
Institute of Physics, Chinese Academy of Sciences, Beijing 100190, China
[2]*University of Chinese Academy of Sciences, Beijing, 100049, China*
[3]*School of Physical Sciences, University of Chinese Academy of Sciences, Beijing 101408, China*
[4]*Collaborative Innovation Center of Quantum Matter, Beijing, China*
[5]*Juelich Centre for Neutron Science (JCNS) at Heinz Maier-Leibnitz Zentrum (MLZ),*
Forschungszentrum Juelich GmbH, Lichtenbergstr. 1, 85747 Garching, Germany
[6]*Helmholtz-Zentrum Dresden-Rossendorf, Institute of Ion Beam Physics and Materials Research,*
Bautzner Landstraße 400, 01328 Dresden, Germany
[7]*State Key Laboratory of Surface Physics, Department of Physics, Fudan University, Shanghai 200433, China*
[8]*Center for Field Theory and Particle Physics, Fudan University, Shanghai 200433, China*
[9]*Laboratory of Advanced Materials, Fudan University, Shanghai 200433, China*
[10]*Collaborative Innovation Center of Advanced Microstructures, Nanjing University, Nanjing 210093, China and*
[11]*Department of Physics, Boston College, Chestnut Hill, Massachusetts 02467, USA*
(Dated: June 1, 2018)

We report the properties of a triangular lattice iron-chalcogenide antiferromagnet FeAl₂Se₄. The spin susceptibility reveals a significant antiferromagnetic interaction with a Curie-Weiss temperature $\Theta_{CW} \simeq -200K$ and a spin-2 local moment. Despite a large spin and a large $|\Theta_{CW}|$, the low-temperature behaviors are incompatible with conventional classical magnets. No long-range order is detected down to 0.4K. Similar to the well-known spin-1 magnet NiGa₂S₄, the specific heat of FeAl₂Se₄ exhibits an unusual double-peak structure and a T^2 power law at low temperatures, which are attributed to the underlying quadrupolar spin correlations and the Halperin-Saslow modes, respectively. The spin freezing occurs at $\sim 14K$, below which the relaxation dynamics is probed by the ac susceptibility. Our results are consistent with the early theory for the spin-1 system with Heisenberg and biquadratic spin interactions. We argue that the early proposal of the quadrupolar correlation and gauge glass dynamics may be well extended to FeAl₂Se₄. Our results provide useful insights about the magnetic properties of frustrated quantum magnets with high spins.

Introduction.—Magnetic frustration arises in systems with competing spin interactions that cannot be optimized simultaneously [1] In general, sufficiently strong frustration could lead to degenerate or nearly degenerate classical spin states and thus induce exotic and unconventional quantum states of matter such as quantum spin liquids when the quantum mechanical nature of the spins is considered. The conventional wisdom and belief tells us that it is more likely to find these quantum states in magnetic systems with spin-1/2 degrees of freedom on frustrated lattices where quantum fluctuations are deemed to be strong. This explains the major efforts and interests in the spin-1/2 triangular lattice magnets like Cs₂CuCl₄ [2, 3], κ-(BEDT-TTF)₂Cu₂(CN)₃ [4–6], EtMe₃Sb[Pd(mit)₂]₂ [7] and YbMgGaO₄ [8–15] the spin-1/2 kagomé lattice magnets like herbertsmithite ZnCu₃(OH)₆Cl₂, volborthite [16] Cu₃V₂O₇(OH)₂·2H₂O and kapellasite [17] Cu₃Zn(OH)₆Cl₂, various spin-1/2 rare-earth pyrochlore magnets [18], and other geometrically frustrated lattices with spin-1/2 moments or effective spin-1/2 moments [19]. Despite the tremendous efforts in the spin-1/2 magnets, the magnets with higher spin moments can occassionally be interesting. The exceptional examples of this kind are the well-known

Haldane phase [20, 21] for the spin-1 chain and its high dimensional extension such as topological paramagnets [22, 23]. The former has been discovered in various Ni-based 1D magnets [24–26]. Another well-known example is the spin-1 triangular lattice antiferromagnet [27–29] NiGa₂S₄, where the biquadratic spin interaction [30–32], that is completely absent for spin-1/2 magnets, bring the spin quadrupolar order/correlation (or spin nematic) physics and phenomena into the system. Therefore, what matters is not just the size of the spin moment, but rather the interactions among the local moments and the underlying lattices.

Inspired by the potentially rich physics in high-spin systems, in this Letter, we study a spin-2 triangular lattice antiferromagnet FeAl₂Se₄ with both polycrystalline and single crystalline samples. Analogous to the Ni²⁺ local moments in NiGa₂S₄ [27–29], the Fe²⁺ local moments in this material form a perfect triangular lattice and provide a perfect setting to explore the quantum physics of high spin moments on frustrated lattice. Unlike the usual classical behaviors expected for high spins, we find that the Fe local moments remain disordered down to 0.4K despite a rather large antiferromagnetic Curie-Weiss temperature $\Theta_{CW} \simeq -200K$. The magnetic

susceptibility of single crystal samples show a bifurcation at about 14K for field cooling and zero-field cooling measurements, suggesting a glassy like spin freezing. This is further assured from the ac susceptibility measurements at different probing frequencies. The specific heat of $FeAl_2Se_4$ shows an unusual double-peak structure at two well-separated temperatures, indicating two distinct physical processes are occurring. Below the spin freezing temperature, a T^2 power law specific heat is observed. Based on the early theoretical works [30–33] on $NiGa_2S_4$, we propose that the double-peak structure in heat capacity arises from the growth of correlation of two distinct types of spin moments, and the T^2 power law is the consequence of the Goldstone-type spin waves (i.e. the Halperin-Saslow modes). We further suggest that the spin freezing is due to the disorder that may induce the gauge glass physics into the would-be ordered state of this system.

Crystal structure.—Our polycrystalline and single crystal $FeAl_2Se_4$ samples were prepared from the high temperature reactions of high purity elements Fe, Al and Se. In Fig. 1(a), we show the room temperature X-ray diffraction pattern on the powder samples that are obtained by grinding the single crystal samples. All the reflections could be indexed with the lattice parameters $a = b = 3.8335(1)$Å, $c = 12.7369(5)$Å, and the unit cell volume $V = 162.108(0.01)$Å^3. The systematic absences are consistent with space group P$\bar{3}$m1 (No. 164), suggesting $FeAl_2Se_4$ is isostructural to the previously reported compound $NiGa_2S_4$ [27]. The structural parameters are listed in Table S1 in the Supplementary material. In Fig. 1(b), we show the X-ray diffraction pattern of the single crystal samples. It clearly indicates that the cleaved surface of the flaky crystal is the (001) plane and normal to the crystallographic c axis. The composition was further examined by inductively coupled plasma atomic emission spectrometer, giving the atomic ratios of Fe: Al: Se close to $1 : 2 : 4$. The compound is built by stacking of layers consisting of edge-sharing $FeSe_6$ octahedra that are connected by a top and a bottom sheet of $AlSe_4$ tetrahedra. The layers are separated with each other by a van der Waals gap. The central $FeSe_6$ octahedra layer is isostructural to the CoO_2 layer of the well-known superconducting material [34] $Na_xCoO_2 \cdot yH_2O$.

In the crystal field environment of $FeAl_2Se_4$, the Fe^{2+} ion has an electronic configuration $t_{2g}^4 e_g^2$ that gives rise to a high spin state and a spin $S = 2$ local moment. The six Fe-Se bonds are of equal length and are $2.609(3)$Å. Se-Fe-Se angles are $94.55(8)°$, marked as α, and $85.45(8)°$, marked as β, as displayed in the inset of Fig. 1(b). The different Se-Fe-Se angles represent a slight rhombohedral distortion of the $FeSe_6$ octahedra, resulting in a small crystal field splitting among the t_{2g} orbitals. The degenerate or nearly degenerate t_{2g} orbitals and the partially filled t_{2g} shell may lead to an active orbital degree of freedom. This will be further discussed from the magnetic
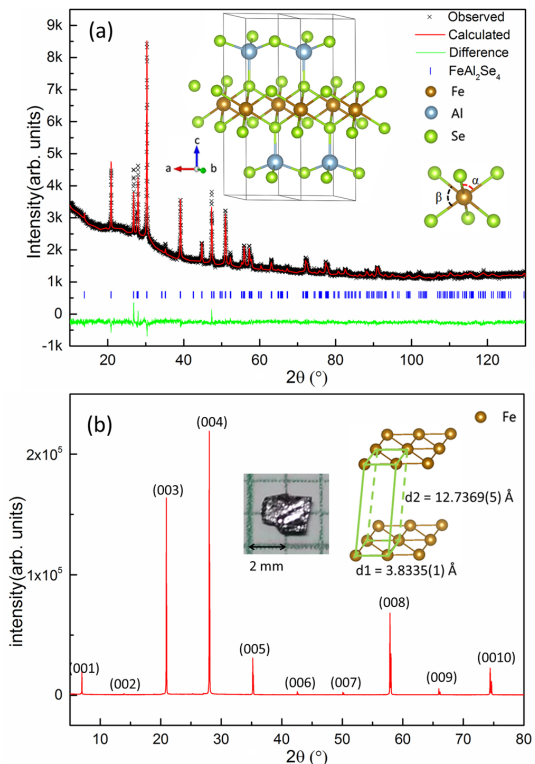

FIG. 1. (Color online.) (a) Powder X-ray diffraction and Ritveld refinement profile of $FeAl_2Se_4$ at the room temperature. The inset shows the schematic crystal structure of $FeAl_2Se_4$ and the distorted $FeSe_6$ octahedra. (b) The X-ray diffraction pattern of $FeAl_2Se_4$ crystal indicates that the (00l) reections dominate the pattern. Inset shows the photography of the $FeAl_2Se_4$ crystal with a length scale of 2 mm and an exhibition of the Fe sublattice.

entropy measurement.

Finally, in $FeAl_2Se_4$, the nearest intralayer Fe-Fe distance is $d_1 = 3.8335(1)$Å and the nearest interlayer Fe-Fe distance is $d_2 = 12.7369(5)$Å, indicating an ideal two-dimensional character in terms of the lattice structure.

Thermodynamic measurements.—To identify the magnetic properties of $FeAl_2Se_4$, we first implement the thermodynamic measurements. The temperature dependent dc magnetic susceptibility and its inverse χ^{-1} under the external magnetic fields of 0.01T, 2T and 8T are shown in Fig. 2. A bifurcation (denoted as T_f) at 14K can be seen under a field of 0.01T, and can be suppressed down to 8K when the applied field is raised up to 8T. This is a signature of spin freezing. The temperature dependent susceptibility from 150K to 300K obeys a simple Curie-Weiss law $\chi = C/(T - \Theta_{CW})$, where C is the Curie constant and Θ_{CW} is the Weiss temperature as illustrated in the inset of Fig. 2(a). The effective magnetic moments, $4.80\text{-}5.20\mu_B$, were obtained from the Curie constants. The Weiss temperature $\Theta_{CW} = -200$K, that is more negative than that for the isostructural material [28] $FeGa_2S_4$ ($\Theta_{CW} = -160$K), indicates stronger
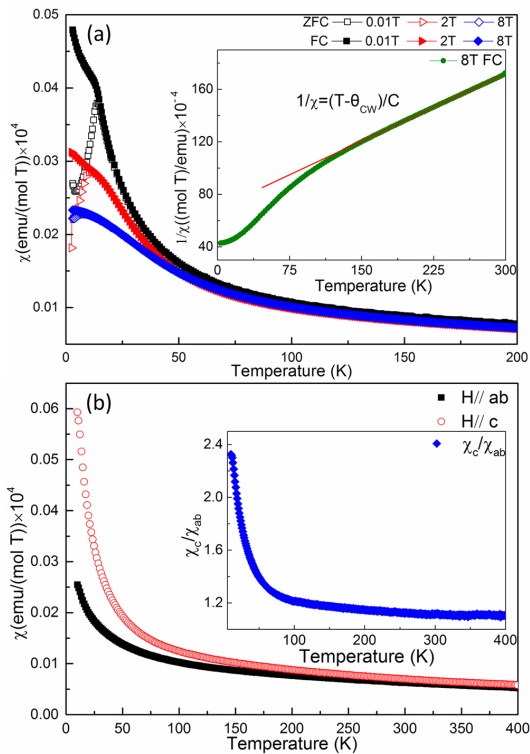
FIG. 2. (Color online.) (a) Zero-field-cold (ZFC) and field-cold (FC) $\chi(T)$ data taken at different applied eld from 2K to 300K. Inset: the inverse susceptibility $\chi^{-1}(T)$ data with the applied field of 8T. The solid red lines are linear fits with a Curie-Weiss law $\chi = C/(T - \Theta_{CW})$. (b) Temperature dependence of the magnetic susceptibility χ_{ab} and χ_c obtained for FeAl$_2$Se$_4$ under 0.1T from 10K to 400K. Inset: the ratio of χ_c/χ_{ab} vs T.

antiferromagnetic interactions. When the temperature is lower than 150K, FeAl$_2$Se$_4$ shows a deviation from the Curie-Weiss behavior. The frustration index, defined by $f = |\Theta_{CW}/T_f|$ with T_f the spin freezing temperature, is estimated as 14. This is a relatively large value, and we thus conclude that FeAl$_2$Se$_4$ is a magnetically frustrated system. In Fig. 2(b) we further show the magnetic susceptibility measurements of the FeAl$_2$Se$_4$ single crystals with $H \parallel ab$ (χ_{ab}) and $H \parallel c$ (χ_c). Unlike NiGa$_2$S$_4$ and FeGa$_2$S$_4$ [28], here we find an easy-axis anisotropy with χ_c/χ_{ab} about 2.4 at 5K instead of easy-plane anisotropy. This is due to the partially filled t_{2g} shell in the Fe^{2+} ion where the spin-orbit coupling is active and induces the anisotropy in the spin space.

The magnetic heat capacity after subtracting the phonon contributions is used to reveal the spin contribution. The heat capacity of an isostructural non-magnetic material ZnIn$_2$S$_4$ is measured to account for the lattice contribution of FeAl$_2$Se$_4$. No clear anomaly associated with any magnetic transition can be detected from the specific heat data down to 0.4K, indicating a ground state without any true long range spin ordering. The

magnetic contribution C_m is obtained by subtracting the phonon contribution from ZnIn$_2$S$_4$. Similar to NiGa$_2$S$_4$ and FeGa$_2$S$_4$ [28], FeAl$_2$Se$_4$ exhibits a double-peak variation of C_m/T: one at ~ 10K, and the other at ~ 65K, as shown in Fig. 3(a). We will revisit the double-peak structure of the heat capacity later.

The magnetic entropy, $S_m(T) = \int_0^T C_m/T \, dT$, increases gradually over the entire measured temperature range but with a plateau near $T \sim 25$K, indicating high degeneracy of low-energy states due to magnetic frustration. The total entropy reaches $R\ln(5)$ at $T \sim 135$K, corresponding to the value for the $S = 2$ system. Then it further increases towards $R\ln(15) = R\ln(5) + R\ln(3)$. The latter term is from the orbital degree of freedom due to two holes present in the t_{2g} orbitals [28]. The low-temperature part of C_m/T, as shown in Fig. 3(b), displays a near linear T dependence around 4K and then deviates from the line with further increasing temperature, similar to the behavior that was observed in NiGa$_2$S$_4$ and FeGa$_2$S$_4$. Besides, the linear-T coefficient γ for C_m/T of 5.9mJ/molK^2 at $T \to 0$K can be obtained for FeAl$_2$Se$_4$, slightly larger than that in FeGa$_2$S$_4$ (3.1mJ/molK^2). The observed T^2 specific heat can be attributed to the Halperin-Saslow modes [35] in two dimensions that give a specific heat of the form

$$C_m = N_A \frac{3\pi k_B V}{c} \Big[\zeta(3) \sum_j \big(\frac{k_B T}{\pi \hbar v_j}\big)^2 - \frac{1}{L_0^2} \Big], \quad (1)$$

where $V = \sqrt{3}a^2c/2$ is the unit-cell volume with a the Fe-Fe spacing, L_0 is the coherence length for the spin excitations and v_j is the velocity in the j-th direction. Using the experimental data on the susceptibility $\chi(T \to 0) = 0.0025$emu/mol and $C_m/T^2 = 0.010$J/molK^3, the estimated spin stiffness $\rho_s = \chi(v/\kappa)^2 = 49.5$K, where $\kappa = g\mu_B/\hbar$, which is larger than those obtained in FeGa$_2$S$_4$ ($\rho_s = 35.8$K) and NiGa$_2$S$_4$ ($\rho_s = 6.5$K). To further compare FeAl$_2$Se$_4$ with the other two counterparts, in the inset of Fig. 3(b) we show $\Delta(C_m/T)\Theta_{CW}/[R\ln(2S + 1)]$ vs T/Θ_{CW} for NiGa$_2$S$_4$ ($S = 1$, $\Theta_{CW} = -80$K), FeGa$_2$S$_4$ ($S = 2$, $\Theta_{CW} = -160$K) and FeAl$_2$Se$_4$ ($S = 2$, $\Theta_{CW} = -200$K) at zero field (0T) in full logarithmic scale, where $\Delta(C_m/T)\Theta_{CW} = C_m/T - \gamma$. As we show in Fig. 3(b), the low-temperature data for FeAl$_2$Se$_4$ nearly collapse on top of NiGa$_2$S$_4$ and FeGa$_2$S$_4$, indicating similar Halperin-Saslow modes present in all three compounds.

Double-peak heat capacity.—Here we discuss the origin of the double-peak structure in the heat capacity of FeAl$_2$Se$_4$. As it was noted, such a double-peak structure was first observed in the spin-1 magnet NiGa$_2$S$_4$ [27]. The theoretical studies have invoked a spin model with both Heisenberg and biquadratic exchange interactions [30–32], where the biquadratic exchange interaction, $-(\boldsymbol{S}_i \cdot \boldsymbol{S}_j)^2$, arises from the spin-lattice coupling. Since FeAl$_2$Se$_4$ is isostructural to NiGa$_2$S$_4$, we
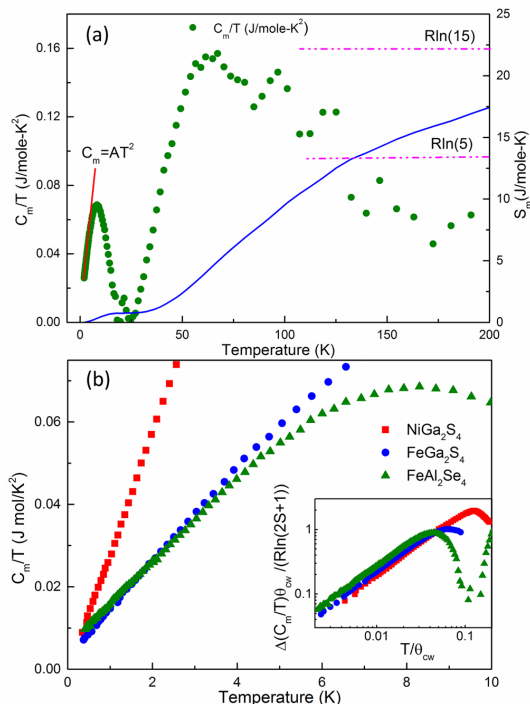
FIG. 3. (Color online.) (a) Temperature dependence of magnetic entropy (right axis) and C_m/T (left axis) for $FeAl_2Se_4$. (b) The low-temperature part of magnetic heat capacity C_m/T for $NiGa_2S_4$, $FeGa_2S_4$ and $FeAl_2Se_4$. Inset shows the $\Delta(C_m/T)\Theta_{CW}/[R\ln(2S+1)]$ vs T/Θ_{CW} for $NiGa_2S_4$ ($S=1$, $\Theta_{CW}=-80K$), $FeGa_2S_4$ ($S=2$, $\Theta_{CW}=-160K$) and $FeAl_2Se_4$ ($S=2$, $\Theta_{CW}=-200K$) at 0T in full logarithmic scale.

expect similar model and interactions to apply. The presence of the biquadratic exchange allows the system to access the spin quadrupole moments effectively and hence enhance the quadrupolar correlation. In addition to the usual magnetic (dipole) moment S^μ, Both spin-1 and spin-2 moments support the quadrupole moments $Q_{\mu\nu} = \frac{1}{2}(S^\mu S^\nu + S^\nu S^\mu) - \frac{1}{3}S(S+1)\delta_{\mu\nu}$ with $\mu = x, y, z$. Since the quadrupole and dipole moments are quite distinct and have different symmetry properties, they ought to behave differently. Moreover, it is the biquadratic interaction that directly couples the quadrupole moments of different sites. It was then argued and shown numerically [30] that the system develops significant quadrupolar correlations at a distinct higher temperature than the one associated with the rapid growth of the magnetic correlations when the system is close to the quantum phase transition from spiral (dipolar) spin order to quadrupolar order. These two temperature scales associated with the rapid growth of magnetic and quadrupolar correlations result in an unusual double-peak structure of the heat capacity. This physics is certainly not unique to the spin-1 $NiGa_2S_4$. Based on the fact that $FeAl_2Se_4$ has an identical lattice structure and an even larger spin Hilbert space, we expect the same mechanism to account for the double-peak heat capacity in $FeAl_2Se_4$.

Spin freezing and ac susceptibility.—To further characterize the low-temperature magnetic properties of $FeAl_2Se_4$ at temperatures near the spin freezing, we measure the temperature dependent ac susceptibility from 5K to 25K for a number of frequencies. As shown in Fig. 4, a peak in the real part at ~ 15 K is present, which is the signature of the susceptibility bifurcation. A small but clear peak shift towards high temperatures can be observed when the probing frequency is increased. This suggests a spin relaxation behavior. The shift of the peak temperature as a function of frequency described by the expression, $(\Delta T_f)/(T_f \Delta \log \omega)$, is usually used to distinguish spin glass and spin glass like materials [36, 37]. The value obtained for $FeAl_2Se_4$ is 0.042, which is slightly larger than expected for a canonical spin glass but is in the range of spin glass like materials. The Volger-Fulcher law is then applied to characterize the relaxation feature with a function relating the bifurcation temperature (T_f) with the frequency (f): $T_f = T_0 - E_a/[k_B \ln(\tau_0 f)]$, where τ_0 is the intrinsic relaxation time, E_a the activation energy of the process, and T_0 "the ideal glass temperature" [38]. The fitted τ_0 is 1×10^{-7}s, which is the same order as the super-paramagnets and cluster glasses. The activation energy of the process E_a is 3.06meV.

Usually the spin freezing with the glassy behavior is due to disorder and/or frustration that are present in $FeAl_2Se_4$. Like the S vacancies in $NiGa_2S_4$, we suspect the Se vacancies to be the dominant type of impurities and sources of disorder. Without disorders, the system may simply develop the spin density or spiral magnetic orders. With (non-magnetic bond) disorders, the phase transition associated with the discrete lattice symmetry breaking would be smeared out in $FeAl_2Se_4$. No sharp transition was observed in the heat capacity measurement on $FeAl_2Se_4$. By assuming a complex XY order parameter for each magnetic domain in the spin freezing regime, the authors in Ref. 30 invoked a phenomenological gauge glass model [39, 40] where the complex orders from different magnetic domains couple with the disorder in a fashion similar to the coupling with a random gauge link variable. They propose that the system would realize a gauge glass ground state, and the Goldstone-type spin waves in a long-range ordered state turn into the Halperin-Saslow modes [33, 35] in the gauge glass model. These gapless modes in two diemnsions contribute to the T^2 specific heat [35] in the spin freezing regime. Due to the phenomenological nature of the model, we think the gauge glass model and the conclusion should also describe and apply to the low-temperature physics in the spin freezing regime of $FeAl_2Se_4$.

Discussion.—Although the large spin moments tend to behave more classically than spin-1/2 moments, the large spin moments have a larger spin Hilbert space and would allow more possibilities for the quantum ground
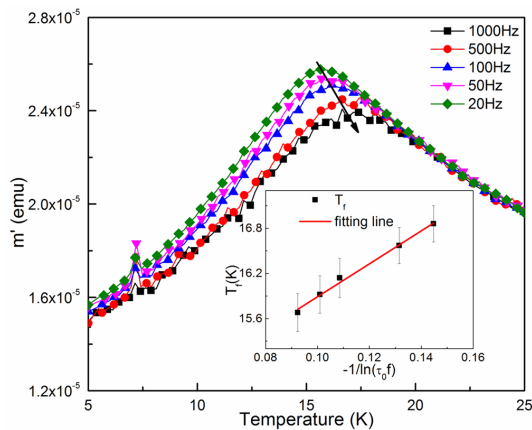
FIG. 4. (Color online.) Temperature dependence of the real part of the ac magnetic susceptibility as a function of frequency. It should be noted that the small peak emerging at approximately 7K in the figure is frequency independent, the origin is unknown.

states. If the interaction can access these Hilbert space effectively, interesting quantum states may be stabilized. From our experimental results in $FeAl_2Se_4$, we find that the system exhibits two-peak structure in the heat capacity. We argue that these two peaks correspond to the separate growth of quadrupolar correlation and magnetic (dipolar) correlation. From the early experience with the spin-1 triangular lattice magnet $NiGa_2S_4$ [27–33], we expect this physics is certainly not specific to $FeAl_2Se_4$, and it is not even specific to spin-2 magnets nor to triangular lattice magnets. This type of physics, i.e. the rich moment structure and their correlations, may broadly exist in frustrated magnets with high spin moments if the interaction can access these high-order multipole moments effectively. In the cases of $FeAl_2Se_4$ and $NiGa_2S_4$, it is the spin-lattice-coupling induced biquadratic interaction that enhances the quadrupolar order and correlation. Besides these two known examples, for other high spin systems such as the $4d/5d$ magnets [41, 42] and $4f$ rare-earth magnets [43–46], the spin-orbit coupling and entanglement could induce strong multipolar interaction and provide another mechanism to access and enhance the quadrupolar (and more generally multipolar) spin orders and correlations. Thus, we think our results and arguments could stimulate interests in frustrated magnets with high spins and rich moment structures.

To be specific to $FeAl_2Se_4$, there are a couple directions for future experiments. Since the biquadratic interaction is suggested to arise from the spin-lattice coupling, it is useful to substitute some Se with S to modify the spin-lattice coupling and hence the biquadratic interaction. This should affect the quadrupolar correlation and the specific heat. Neutron scattering measurement can be quite helpful to probe both the low-energy modes like the Halperin-Saslow modes and the spin correlation in different temperature regimes [47]. Nuclear magnetic resonance and muon spin resonance experiments can also be useful to reveal the dynamical properties of the system at different temperatures. On the theoretical side, it would be interesting to establish a general understanding and a phase diagram of a spin-2 model with both Heisenberg and biquadratic interactions on the triangular lattice.

* wangzi@bc.edu
† gangchen.physics@gmail.com
‡ chenx29@iphy.ac.cn

[1] Leon Balents, "Spin liquids in frustrated magnets," Nature **464**, 199–208 (2010).
[2] R. Coldea, D. A. Tennant, and Z. Tylczynski, "Extended scattering continua characteristic of spin fractionalization in the two-dimensional frustrated quantum magnet Cs_2CuCl_4 observed by neutron scattering," Phys. Rev. B **68**, 134424 (2003).
[3] R. Coldea, D. A. Tennant, A. M. Tsvelik, and Z. Tylczynski, "Experimental Realization of a 2D Fractional Quantum Spin Liquid," Phys. Rev. Lett. **86**, 1335–1338 (2001).
[4] Y. Shimizu, K. Miyagawa, K. Kanoda, M. Maesato, and G. Saito, "Spin Liquid State in an Organic Mott Insulator with a Triangular Lattice," Phys. Rev. Lett. **91**, 107001 (2003).
[5] Y. Kurosaki, Y. Shimizu, K. Miyagawa, K. Kanoda, and G. Saito, "Mott Transition from a Spin Liquid to a Fermi Liquid in the Spin-Frustrated Organic Conductor κ-$(ET)_2Cu_2(CN)_3$," Phys. Rev. Lett. **95**, 177001 (2005).
[6] Satoshi Yamashita, Yasuhiro Nakazawa, Masaharu Oguni, Yugo Oshima, Hiroyuki Nojiri, Yasuhiro Shimizu, Kazuya Miyagawa, and Kazushi Kanoda, "Thermodynamic properties of a spin-1/2 spin-liquid state in a kappa-type organic salt," Nature Physics **4**, 459–462 (2008).
[7] T Itou, A Oyamada, S Maegawa, M Tamura, and R Kato, "Spin-liquid state in an organic spin-1/2 system on a triangular lattice, $EtMe_3Sb[Pd(dmit)_2]_2$," Journal of Physics: Condensed Matter **19**, 145247 (2007).
[8] Yuesheng Li, Haijun Liao, Zhen Zhang, Shiyan Li, Feng Jin, Langsheng Ling, Lei Zhang, Youming Zou, Li Pi, Zhaorong Yang, Junfeng Wang, Zhonghua Wu, and Qingming Zhang, "Gapless quantum spin liquid ground state in the two-dimensional spin-1/2 triangular antiferromagnet YbMgGaO4," Scientific Reports **5**, 16419 (2015).
[9] Yuesheng Li, Gang Chen, Wei Tong, Li Pi, Juanjuan Liu, Zhaorong Yang, Xiaoqun Wang, and Qingming Zhang, "Rare-Earth Triangular Lattice Spin Liquid: A Single-Crystal Study of $YbMgGaO_4$," Phys. Rev. Lett. **115**, 167203 (2015).
[10] Yao Shen, Yao-Dong Li, Hongliang Wo, Yuesheng Li,

Shoudong Shen, Bingying Pan, Qisi Wang, H. C. Walker, P. Steffens, M Boehm, Yiqing Hao, D. L. Quintero-Castro, L. W. Harriger, Lijie Hao, Siqin Meng, Qingming Zhang, Gang Chen, and Jun Zhao, "Spinon Fermi surface in a triangular lattice quantum spin liquid YbMgGaO$_4$," Nature **540**, 559–562 (2016).

[11] Joseph A. M. Paddison, Zhiling Dun, Georg Ehlers, Yaohua Liu, Matthew B. Stone, Haidong Zhou, and Martin Mourigal, "Continuous excitations of the triangular-lattice quantum spin liquid YbMgGaO$_4$," Nature Physics **13**, 117–122 (2017).

[12] Yao-Dong Li, Yuan-Ming Lu, and Gang Chen, "Spinon Fermi surface $U(1)$ spin liquid in the spin-orbit-coupled triangular-lattice Mott insulator YbMgGaO$_4$," Phys. Rev. B **96**, 054445 (2017).

[13] Jason Iaconis, Chunxiao Liu, Gbor B. Halsz, and Leon Balents, "Spin Liquid versus Spin Orbit Coupling on the Triangular Lattice," SciPost Phys. **4**, 003 (2018).

[14] Zhenyue Zhu, P. A. Maksimov, Steven R. White, and A. L. Chernyshev, "Disorder-Induced Mimicry of a Spin Liquid in YbMgGaO$_4$," Phys. Rev. Lett. **119**, 157201 (2017).

[15] Yao-Dong Li, Yao Shen, Yuesheng Li, Jun Zhao, and Gang Chen, "Effect of spin-orbit coupling on the effective-spin correlation in YbMgGaO$_4$," Phys. Rev. B **97**, 125105 (2018).

[16] Zenji Hiroi, Masafumi Hanawa, Naoya Kobayashi, Minoru Nohara, Hidenori Takagi, Yoshitomo Kato, and Masashi Takigawa, "Spin-1/2 Kagom-Like Lattice in Volborthite Cu$_3$V$_2$O$_7$(OH)$_2$2H$_2$O," Journal of the Physical Society of Japan **70**, 3377–3384 (2001).

[17] B. Fåk, E. Kermarrec, L. Messio, B. Bernu, C. Lhuillier, F. Bert, P. Mendels, B. Koteswararao, F. Bouquet, J. Ollivier, A. D. Hillier, A. Amato, R. H. Colman, and A. S. Wills, "Kapellasite: A Kagome Quantum Spin Liquid with Competing Interactions," Phys. Rev. Lett. **109**, 037208 (2012).

[18] Jason S. Gardner, Michel J. P. Gingras, and John E. Greedan, "Magnetic pyrochlore oxides," Rev. Mod. Phys. **82**, 53–107 (2010).

[19] Yoshihiko Okamoto, Minoru Nohara, Hiroko Aruga-Katori, and Hidenori Takagi, "Spin-Liquid State in the $S = 1/2$ Hyperkagome Antiferromagnet Na$_4$Ir$_3$O$_8$," Phys. Rev. Lett. **99**, 137207 (2007).

[20] F. D. M. Haldane, "Nonlinear Field Theory of Large-Spin Heisenberg Antiferromagnets: Semiclassically Quantized Solitons of the One-Dimensional Easy-Axis Néel State," Phys. Rev. Lett. **50**, 1153–1156 (1983).

[21] Ian Affleck, Tom Kennedy, Elliott H. Lieb, and Hal Tasaki, "Rigorous results on valence-bond ground states in antiferromagnets," Phys. Rev. Lett. **59**, 799–802 (1987).

[22] Xie Chen, Zheng-Cheng Gu, Zheng-Xin Liu, and Xiao-Gang Wen, "Symmetry-Protected Topological Orders in Interacting Bosonic Systems," Science **338**, 1604–1606 (2012).

[23] Chong Wang, Adam Nahum, and T. Senthil, "Topological paramagnetism in frustrated spin-1 Mott insulators," Phys. Rev. B **91**, 195131 (2015).

[24] W. J. L Buyers, R. M. Morra, R. L. Armstrong, M. J. Hogan, P. Gerlach, and K. Hirakawa, "Experimental evidence for the Haldane gap in a spin-1 nearly isotropic, antiferromagnetic chain," Phys. Rev. Lett. **56**, 371–374 (1986).

[25] Yoshitami Ajiro, Tsuneaki Goto, Hikomitsu Kikuchi, Toshiro Sakakibara, and Toshiya Inami, "High-field magnetization of a quasi-one-dimensional S=1 antiferromagnet Ni(C$_2$H$_8$N$_2$)$_2$NO$_2$(ClO$_4$: Observation of the Haldane gap," Phys. Rev. Lett. **63**, 1424–1427 (1989).

[26] A. P. Ramirez, S-W. Cheong, and M. L. Kaplan, "Specific heat of defects in Haldane systems Y$_2$BaNiO$_5$ and NENP: Absence of free spin-1/2 excitations," Phys. Rev. Lett. **72**, 3108–3111 (1994).

[27] Satoru Nakatsuji, Yusuke Nambu, Hiroshi Tonomura, Osamu Sakai, Seth Jonas, Collin Broholm, Hirokazu Tsunetsugu, Yiming Qiu, and Yoshiteru Maeno, "Spin disorder on a triangular lattice," Science **309**, 1697–1700 (2005).

[28] S. Nakatsuji, H. Tonomura, K. Onuma, Y. Nambu, O. Sakai, Y. Maeno, R. T. Macaluso, and Julia Y. Chan, "Spin Disorder and Order in Quasi-2D Triangular Heisenberg Antiferromagnets: Comparative Study of FeGa$_2$S$_4$, Fe$_2$Ga$_2$S$_5$, and NiGa$_2$S$_4$," Phys. Rev. Lett. **99**, 157203 (2007).

[29] C. Stock, S. Jonas, C. Broholm, S. Nakatsuji, Y. Nambu, K. Onuma, Y. Maeno, and J.-H. Chung, "Neutron-Scattering Measurement of Incommensurate Short-Range Order in Single Crystals of the $S = 1$ Triangular Antiferromagnet NiGa$_2$**S**$_4$," Phys. Rev. Lett. **105**, 037402 (2010).

[30] E. M. Stoudenmire, Simon Trebst, and Leon Balents, "Quadrupolar correlations and spin freezing in $S = 1$ triangular lattice antiferromagnets," Phys. Rev. B **79**, 214436 (2009).

[31] Subhro Bhattacharjee, Vijay B. Shenoy, and T. Senthil, "Possible ferro-spin nematic order in NiGa$_2$S$_4$," Phys. Rev. B **74**, 092406 (2006).

[32] Hirokazu Tsunetsugu and Mitsuhiro Arikawa, "Spin nematic phase in s=1 triangular antiferromagnets," Journal of the Physical Society of Japan **75**, 083701 (2006).

[33] Daniel Podolsky and Yong Baek Kim, "Halperin-Saslow modes as the origin of the low-temperature anomaly in NiGa$_2$S$_4$," Phys. Rev. B **79**, 140402 (2009).

[34] R. E. Schaak, T. Klimczuk, M. L. Foo, and R. J. Cava, "Superconductivity phase diagram of na$_x$coo$_2$1.3h$_2$o," Nature **424**, 527–529 (2003).

[35] B. I. Halperin and W. M. Saslow, "Hydrodynamic theory of spin waves in spin glasses and other systems with non-collinear spin orientations," Phys. Rev. B **16**, 2154–2162 (1977).

[36] J. A. Mydosh, *Spin Glasses: An Experimental Introduction* (CRC, 1993).

[37] J. W. Krizan and R. J. Cava, "NaCaCo$_2$F$_7$: A single-crystal high-temperature pyrochlore antiferromagnet," Phys. Rev. B **89**, 214401 (2014).

[38] T Klimczuk, H W Zandbergen, Q Huang, T M McQueen, F Ronning, B Kusz, J D Thompson, and R J Cava, "Cluster-glass behavior of a highly oxygen deficient perovskite, BaBi$_{0.28}$Co$_{0.72}$O$_{2.2}$," Journal of Physics: Condensed Matter **21**, 105801 (2009).

[39] Daniel S. Fisher and David A. Huse, "Equilibrium behavior of the spin-glass ordered phase," Phys. Rev. B **38**, 386–411 (1988).

[40] Daniel S. Fisher, Matthew P. A. Fisher, and David A. Huse, "Thermal fluctuations, quenched disorder, phase transitions, and transport in type-ii superconductors," Phys. Rev. B **43**, 130–159 (1991).

[41] Gang Chen, Rodrigo Pereira, and Leon Balents, "Exotic

phases induced by strong spin-orbit coupling in ordered double perovskites," Phys. Rev. B **82**, 174440 (2010).

[42] Gang Chen and Leon Balents, "Spin-orbit coupling in d^2 ordered double perovskites," Phys. Rev. B **84**, 094420 (2011).

[43] Shigeki Onoda and Yoichi Tanaka, "Quantum melting of spin ice: Emergent cooperative quadrupole and chirality," Phys. Rev. Lett. **105**, 047201 (2010).

[44] Yi-Ping Huang, Gang Chen, and Michael Hermele, "Quantum spin ices and topological phases from dipolar-octupolar doublets on the pyrochlore lattice," Phys. Rev. Lett. **112**, 167203 (2014).

[45] Yao-Dong Li, Xiaoqun Wang, and Gang Chen, "Hidden multipolar orders of dipole-octupole doublets on a triangular lattice," Phys. Rev. B **94**, 201114 (2016).

[46] Changle Liu, Yao-Dong Li, and Gang Chen, "Selective measurements of intertwined multipolar orders: non-Kramers doublets on a triangular lattice," arXiv **1805.01865**.

[47] Andrew Smerald, Hiroaki T. Ueda, and Nic Shannon, "Theory of inelastic neutron scattering in a field-induced spin-nematic state," Phys. Rev. B **91**, 174402 (2015).